

Supplemental Information

Figure S1 related to Figure 2

(shows TNF release, epigenetic changes in the *Nos2* gene and analysis of macrophage signalling pathways upon high salt stress)

Figure S2 related to Figure 3

(shows p38/ MAPK and NFAT5 mediated HS-boost of NO release from LPS-stimulated bone marrow-derived macrophages)

Figure S3 related to Figure 4

(shows NFAT5 protein level and NO production in macrophages derived from bone marrow of $\text{LysM}^{\text{Cre}} \text{Nfat5}^{\text{fl/fl}}$ and $\text{LysM}^{\text{WT}} \text{Nfat5}^{\text{fl/fl}}$ mice)

Table S1 & S2 related to Figure 2

(shows Na^+ content and osmolality in macrophage cell culture and quality metrics of ChIP-seq)

Supplemental experimental procedures

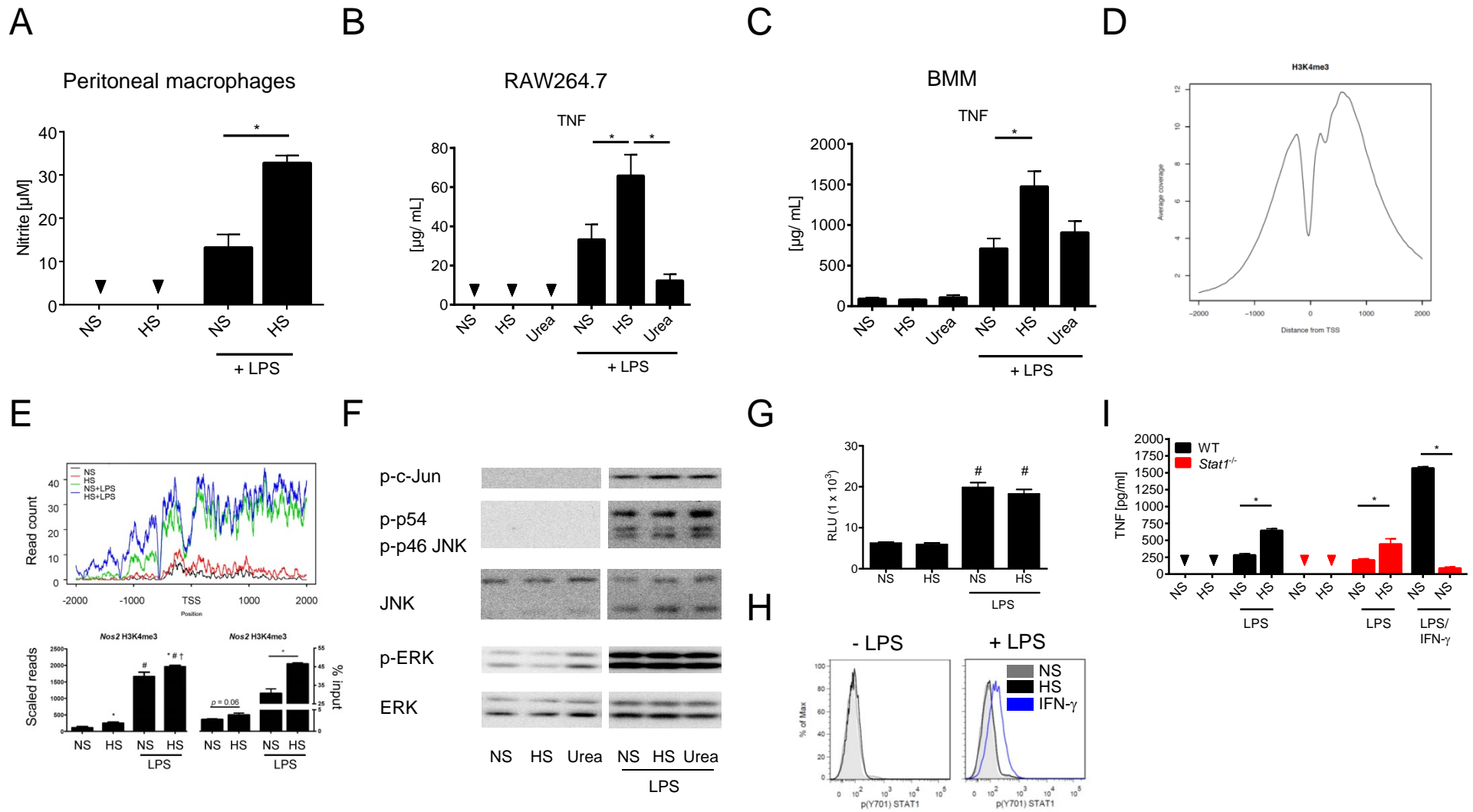
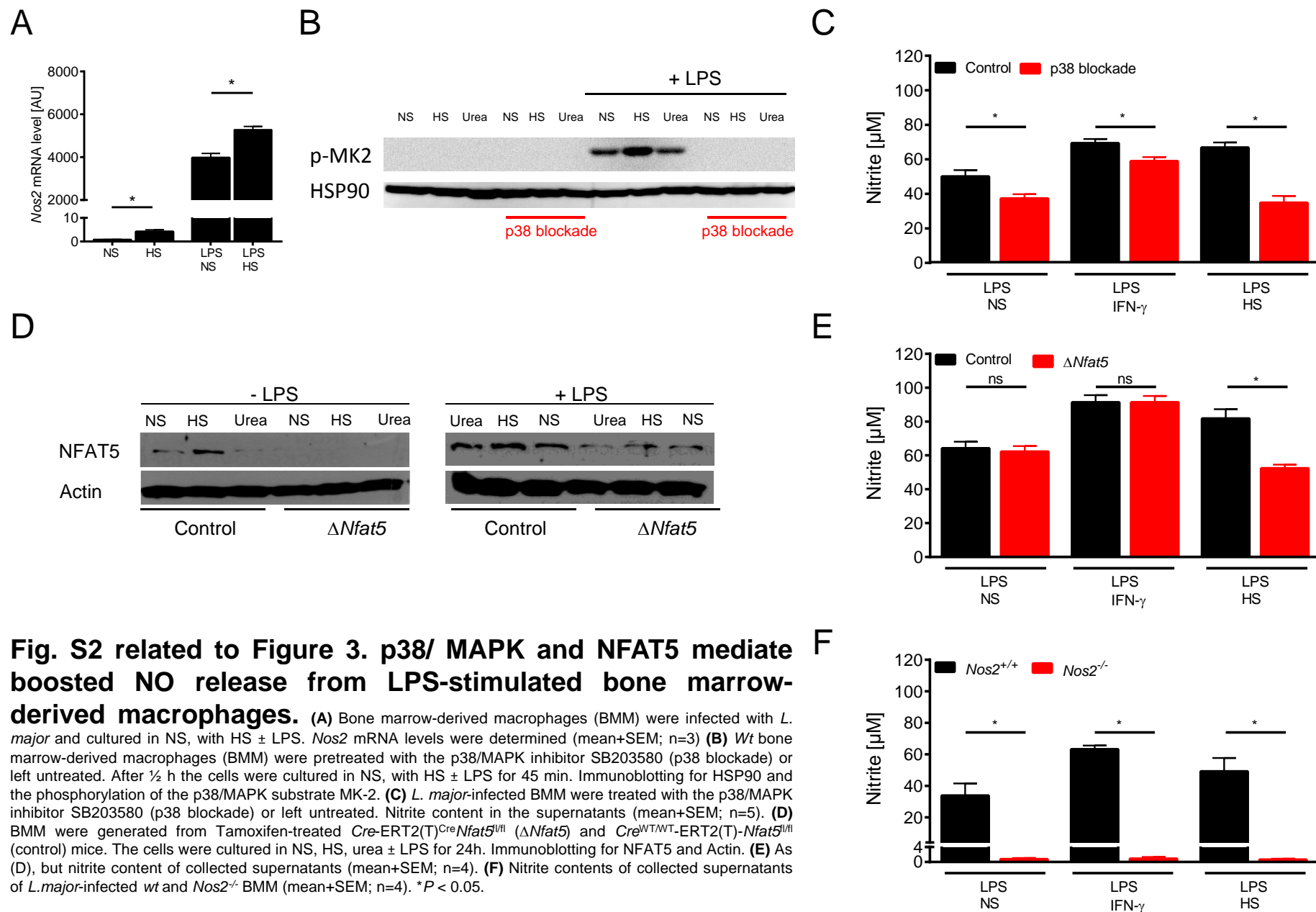


Fig. S1 related to Figure 2. High salt-induced effects on macrophage activation. (A) 24 h after indicated stimulation, nitrite was determined in supernatants of peritoneal macrophages (mean+SEM; n=2 performed in quadruplicates). * $P < 0.05$ (B & C) 24 h after indicated stimulation, tumor necrosis factor (TNF) levels were analyzed in the supernatant of RAW 264.7 macrophages (mean+SEM; n=4) and BMM (mean+SEM; n=3). * $P < 0.05$ (D) Average coverage of histone modification ChIP-seq reads around all annotated transcription start site (TSS) for histone H3 lysine 4 trimethylation (H3K4me3). (E) Histone modification ChIP-seq reads around *Nos2* transcription start site (TSS). Upper panel, mean coverage of histone H3 lysine 4 trimethylation (H3K4me3) 2000 bp up- and downstream of the *Nos2* TSS for NS and HS \pm LPS (10ng/ml). Lower left panel, corresponding bar graph (reads normalized for library size; mean+SEM; n=3). * $P(\text{HS}) < 0.05$; # $P(\text{LPS}) < 0.05$; † $P(\text{LPS}*\text{HS}) < 0.05$. Lower right panel, ChIP-qPCR confirmation of enriched H3K4me3 in the *Nos2* promoter (mean+SEM; n=3). * $P < 0.05$. (F) Activation of JNK, c-Jun and ERK was analyzed in RAW 264.7 macrophages 45 min after indicated stimulation. Representative immunoblots out of at least three independent experiments are given. (G) After 2 h of stimulation, NF- κB activity was assessed by determination of the luciferase activity of RAW- κB cell lysates. A representative experiment in quintuplicates out of two similar experiments is given (mean+SEM). # $P(\text{LPS}) < 0.05$ (H) After 30 min of indicated stimulation, phosphorylation of STAT1 at Tyr 701 was analyzed by flow cytometry. A representative out of two similar experiments is displayed. (I) BMM from *Stat1*^{-/-} and littermate controls were stimulated as indicated. After 24 h, TNF in the supernatants was assessed (mean+SEM; a representative of two similar experiments in triplicates); Triangles: not detectable. * $P < 0.05$



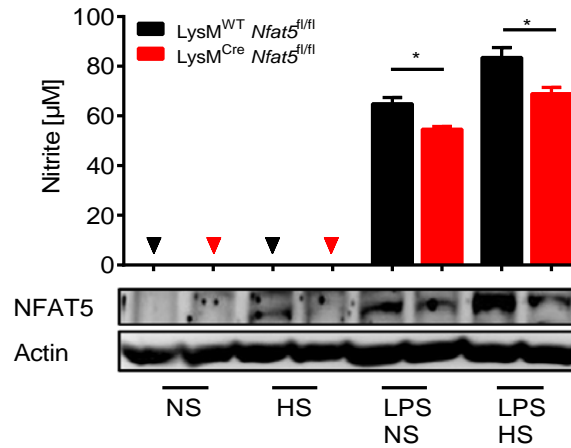


Fig. S3 NFAT5 protein level and NO production in macrophages derived from bone marrow of LysM^{CRE} Nfat5^{fl/fl} and LysM^{WT} Nfat5^{fl/fl} mice

Bone marrow-derived macrophages from LysM^{WT}Nfat5^{fl/fl} and LysM^{Cre} Nfat5^{fl/fl} were cultured in normal cell culture medium (NS: normal salt), with additional 40 mM NaCl in the medium (HS: high salt) ± LPS (10 ng/ml) for 24 h. Upper panel: Nitrite levels in the supernatants (mean+SEM; n=3); Triangles: not detectable. **P* < 0.05; Lower panel: Immunoblotting for NFAT5 and Actin.

Table S1 related to Figure 2. Na⁺ content and osmolality in macrophage cell culture. RAW 264.7 macrophages were cultured in normal cell culture medium (NS: normal salt), with additional 40 mM NaCl in the medium (HS: high salt) or 80 mM urea ± 10 ng/ml LPS for 24 h. Osmolality and Na⁺ concentrations of the supernatants were analyzed (means ± SD). *P* (vs. NS) < 0.05.

	NS	HS	Urea	NS & LPS	HS & LPS	Urea & LPS
Osmolality [mosm/ kg]	299 ± 3	381 ± 4*	383 ± 1*	299 ± 4	381 ± 1*	378 ± 6*
Na ⁺ [mmol/l]	141 ± 2	173 ± 3*	137 ± 3	142 ± 2	182 ± 19*	139 ± 2

Table S2 related to Figure 2. ChIP-seq quality metrics. As defined in the ENCODE consortium (Landt et al. 2012), quality metrics were computed using the SPP tool. NSC: normalized strand cross correlation, RSC: relative strand cross correlation. All experiments yielded the best possible quality tags.

	Filename	numReads	estFragLen	corr_estFragLen	NSC	RSC	QualityTag
NS	Sample_H3K4me3-con1-bio1-tech1.bam	48958784	150	0.5059	1.849	3.552	2
NS	Sample_H3K4me3-con1-bio2-tech1.bam	29441783	150	0.4664	1.875	6.199	2
NS	Sample_H3K4me3-con1-bio3-tech1.bam	41636837	150	0.5103	1.964	4.287	2
HS	Sample_H3K4me3-con2-bio1-tech1.bam	60490146	145	0.5192	1.815	2.992	2
HS	Sample_H3K4me3-con2-bio2-tech1.bam	27989643	150	0.4860	2.031	6.960	2
HS	Sample_H3K4me3-con2-bio3-tech1.bam	46633261	150	0.5109	1.930	3.957	2
LPS	Sample_H3K4me3-con4-bio1-tech1.bam	40073783	145	0.5012	1.842	3.416	2
LPS	Sample_H3K4me3-con4-bio2-tech1.bam	27560633	145	0.4637	1.768	4.444	2
LPS	Sample_H3K4me3-con4-bio3-tech1.bam	39865326	145	0.4922	1.758	3.382	2
LPS HS	Sample_H3K4me3-con5-bio1-tech1.bam	59845456	130.145	0.5116/0.5102	1.655	3.002	2
LPS HS	Sample_H3K4me3-con5-bio2-tech1.bam	28271259	150	0.4693	1.745	5.939	2
LPS HS	Sample_H3K4me3-con5-bio3-tech1.bam	47028466	145	0.5002	1.690	3.185	2
NS	Sample_H4ac-con1-bio1-tech1.bam	78999383	145	0.5368	1.276	6.575	2
NS	Sample_H4ac-con1-bio2-tech1.bam	43234549	130.145	0.4364/0.4321	1.274	8.530	2
NS	Sample_H4ac-con1-bio3-tech1.bam	45050178	150	0.4626	1.330	15.963	2
HS	Sample_H4ac-con2-bio1-tech1.bam	81529474	130.145	0.5480/0.5463	1.257	4.539	2
HS	Sample_H4ac-con2-bio2-tech1.bam	50115023	145	0.4628	1.204	14.004	2
HS	Sample_H4ac-con2-bio3-tech1.bam	42127753	150	0.4769	1.420	9.218	2
LPS	Sample_H4ac-con4-bio1-tech1.bam	47553959	145	0.4523	1.277	7.102	2
LPS	Sample_H4ac-con4-bio2-tech1.bam	45489641	130.145	0.4405/0.4368	1.195	5.640	2
LPS	Sample_H4ac-con4-bio3-tech1.bam	42584777	145	0.4375	1.235	5.934	2
LPS HS	Sample_H4ac-con5-bio1-tech1.bam	67213581	130.145	0.5166/0.5111	1.258	5.004	2
LPS HS	Sample_H4ac-con5-bio2-tech1.bam	47548734	145	0.4632	1.262	10.374	2
LPS HS	Sample_H4ac-con5-bio3-tech1.bam	46501814	145	0.4687	1.278	7.373	2
	Sample_input-mix-bio1-tech1.bam	62502414	150.340.530	0.4718/0.4611/0.4598	1.039	2.470	2

Supplemental Experimental Procedures

Reagents

p38/MAPK blocker SB203580 and LPS (*E.coli* O111:B4) were purchased from Sigma-Aldrich and Invivogen. Urea and NaCl were purchased from VWR. No endotoxin was detected in the urea and NaCl stock solutions that were used in the cell culture experiments as determined by the Limulus Amebocyte Lysate assay (QCL-1000, Cambrex, detection limit: 10 pg LPS/ml). Recombinant murine IFN- γ and TNF were purchased from eBiosciences. Recombinant mouse IL-1 α und IL-1 β was purchased from RnD Systems. Non-silencing siRNA oligonucleotides, and siRNA-duplexes directed against *Nfat5* (L-058868-01-0020) were purchased from Qiagen and Thermo Scientific, respectively.

Antibodies

For immunblotting, the following antibodies were used: rabbit anti-actin (Sigma-Aldrich); rabbit-anti-HSP 90 α/β (Santa Cruz), rabbit anti-NFAT5/ TonEBP (Thermo Scientific), anti-p38/MAPK (Cell Signaling Technology via New England Biolabs), anti-p-p38/MAPK (T180/Y182; Cell Signaling Technology), rabbit anti-p-MAPKAPK-2 (Thr334; Cell Signaling Technology), rabbit anti-MAPKAPK-2 (MK2; Cell Signaling Technology), rabbit anti-p44/42 (ERK1/2; Cell Signaling Technology), rabbit p-p44/42 MAPK (ERK1/2; Thr202/Tyr204; Cell Signaling Technology), rabbit anti-SAPK/JNK (Cell Signaling Technology), rabbit anti p-SAPK/JNK (Thr183/Tyr185; Cell Signaling Technology), rabbit anti p-c-Jun (Ser73, Cell Signaling Technology), PE mouse anti-STAT1 (pY701, BD Biosciences), FITC mouse anti-NOS2 (BD Biosciences), APC rat-anti-CD11b (eBiosciences), rat anti mouse CD68 (AbDserotec).

Parasites

Promastigotes of the *L. major* strain MHOM/IL/81/FE/BNI (Stenger et al., 1996) were derived from skin lesions of BALB/c mice and propagated *in vitro* in RPMI 1640 (10% fetal calf serum) on Novy-Nicolle-MacNeal blood agar slants for a maximum of five passages.

Macrophages

RAW 246.7 macrophages (American Type Culture Collection), and RAW 246.7 macrophages that overexpress *Nfat5* and RAW 246.7 harboring a stable NF- κ B reporter (RAW- κ B) were used as described earlier (Machnik et al., 2009; Wittmann et al., 2008). Bone marrow-derived macrophages (BMM) from C57BL/6 mice (Charles River), *Stat1*-deficient (Neufert et al.,

2007), *Nos2*-deficient mice (B6;129P2-*Nos2tm1Lau/J41* mice (The Jackson Laboratory, Bar Harbor, USA) were prepared in hydrophobic Teflon[®] bags (FT FEP 100 C (DuPont), American Durafilm, Holliston, USA) as described earlier (Schleicher and Bogdan, 2009; Wiese et al., 2010). For generation of *Nfat5*-deficient BMM, the Tamoxifen-inducible Cre-deleter mouse strain B6.Cg-Tg(UBC-cre/ERT2)1Ejb/J (Ruzankina et al., 2007) (The Jackson Laboratory) was crossed with *Nfat5*^{fl/fl} mice, that harbor two *loxP* sites which target exon 4 of the *Nfat5* gene as described earlier (Kueper, 2013; Wiig et al., 2013). The offspring with the genotype *Cre-ERT2(T)*^{Cre} *Nfat5*^{fl/fl} and *Cre-ERT2(T)*^{WT/WT} *Nfat5*^{fl/fl} was fed for ~28 days with a diet containing 400 mg Tamoxifen/ kg (LASCRdiet CreActive TAM400, Lasvendi) to generate inducible NFAT5-deficient or control mice. To delete p38 α , Mx^{WT} p38 α ^{fl/fl} (control) and Mx^{CRE} p38 α ^{fl/fl} (Δ p38 α) mice were injected three times i.p. at week 5 with poly I:C (13 mg/kg body weight) as described earlier (Bohm et al., 2009).

Nitrite and TNF production

Nitrite accumulation in the supernatant was used as an indicator of NO production and was determined by the Griess reaction using sodium nitrite as a standard. Mouse TNF was analyzed from the supernatant of stimulated cells by a standard sandwich ELISA technique using matched Ab pairs according to the manufacturer's recommendations (BD Opt-EIA[™], BD Biosciences).

Analysis of STAT1-phosphorylation by flow cytometry

STAT1 activation was analyzed by flow cytometry after performing a staining for intracellular phosphorylated STAT1 using PE mouse anti-STAT1 (pY701) antibody after fixation of the single cells with paraformaldehyde and permeabilization with BD Phosflow[™] Perm Buffer IV (BD Biosciences). Data acquisition was performed using a FACS Canto II (BD Biosciences) and data were analyzed with FlowJo software (Tree Star).

NF- κ B reporter activity

Stimulated RAW- κ B cells were lysed with a suitable lysis buffer (PBS, 2mM EDTA, 1% TritonX-100 and 10% glycerine) and processed with luciferase substrate (Promega) as described earlier (Wittmann et al., 2008).

RNA isolation, reverse transcription, real-time PCR and relative quantification

Total RNA from cell culture experiments was extracted with Trifast[®] (PeqLab, Erlangen, Germany) according to the manufacturer's instruction, reverse transcribed using the High Capacity cDNA Archive kit (Applied Biosystems) and analyzed by real-time quantitative RT-PCR (qRT-PCR) on an ABI Prism 7900 sequence detector (Applied Biosystems) using Taqman Universal Mastermix and Assays-on-Demand (Applied Biosystems) as described earlier (Jantsch et al., 2011). The following assays were used: murine hypoxanthine guanine phosphoribosyl transferase 1 (Mm00446969_m1), type-2 nitric oxide synthase (miNOS; Mm00440485_m1). Data were analyzed using the $\Delta\Delta C_T$ method. The normalized ratio of target mRNA *Nos2* to the internal control mRNA *Hprt1* was set to 1.

RNA interference in macrophages

RNA interference was performed as described earlier (Machnik et al., 2009; Wiese et al., 2010). Briefly, macrophages were harvested, resuspended in Opti-MEM, transferred together with the respective siRNA duplexes to a 4-mm cuvette and pulsed in a Gene Pulser Xcell (400V, 150 μ F, 100 Ω). Transfection efficiency was > 90%. Two days after transfer of siRNA, macrophages were subjected to the experimental conditions.

Immunoblotting

At indicated time-points macrophage monolayers were lysed using a PE-lysis buffer (6,65 M Urea, 10% Glycerine, 1% SDS, Tris [tris(hydroxymethyl)aminomethane] HCl, pH 6.8, 5 mM DTT) for detection of NFAT5 and supplemented with a protease inhibitor cocktail (Roche Diagnostics) directly before use. For detection of MAPK, we used a modified Ripa-lysis buffer (1% Igepal CA-630, 0.1% sodium deoxycholate, 150 mM sodium chloride, 1 mM EDTA, 50 mM Tris (pH 7.5), supplemented with a protease and a phosphatase inhibitor cocktail (Roche Diagnostics) directly before use). Lysates were diluted with SDS-PAGE sample buffer and separated by sodium dodecyl sulfate (SDS)-polyacrylamide gel electrophoresis and transferred onto polyvinylidene difluoride membrane (Millipore). Proteins were detected by specific antibodies. The bound antibodies were visualized by ECL technology. Densitometry was performed with ImageJ (version 1.47, National Institutes of Health).

Chromatin Immunoprecipitation (ChIP) and Sequencing

We performed 12 ChIP-seq experiments to determine histone modification (H3K4me3) levels of murine primary BMM after 24h LPS (10ng/ml) stimulation in the presence or absence of 40 mM NaCl. The protocol was modified from (Barski et al., 2007). Briefly, 40×10^6 BMM per group (NS, HS, LPS, LPS HS) were used to isolate nuclei by centrifugation through a dense sucrose cushion. Subsequently, samples were digested with micrococcal nuclease (Sigma-Aldrich) to generate native chromatin templates consisting mainly of mononucleosomes. Chromatin was precipitated over night at 4°C with anti-H3K4me3 (New England Biolabs, 9751 S) bound to Dynabeads® Protein A (Invitrogen, 10002D). MinElute PCR Purification Kit (QIAGEN) was used to purify immunoprecipitated DNA after proteinase K (Sigma-Aldrich) digestion; specificity of immunoprecipitation was confirmed with known active and inactive genes by qPCR.

50 ng of purified DNA was used to construct ChIP-seq libraries according to the manufacturer's protocol (Illumina/ Solexa). After cluster generation, sequencing was performed using the Illumina HiSeq 2000 platform. In addition we performed independent ChIP experiments as described above to confirm our findings on histone modification levels (H3K4me3) at the transcription start site of *Nos2* by quantitative PCR. We used primers musNos2-ChIP-2-for: 5'AACCTCACTGAGAGAACAGACAGAAA3' musNos2-ChIP-2-rev: 5'TTGCAGCTGCTGAGGGATT3' to amplify a genomic fragment a short distance upstream from the annotated transcription start site of *Nos2*. Data were normalized as percent of input as follows: $100 * 2^{(\text{Adjusted input} - \text{Ct (IP)})}$.

Alignment of ChIP-seq data

Short reads were mapped to the mouse reference genome (mm9) using the bowtie algorithm retaining only reads that map uniquely to the genome with at most 2 mismatches in the seed sequence. For each sample we removed duplicated reads that are likely PCR amplification artifacts using SAMtools (Li et al., 2009).

Quality assessment of ChIP-seq data

We assessed the quality of our ChIP-seq data using metrics developed by the ENCODE consortium (Landt et al., 2012) which is summarized in **Table S2**. For quality control we generated read coverage plots in regions of 4 kb around annotated transcription start site (TSS) (**Figure S1D**) similar to Barski *et al* (Barski et al., 2007).

Quantification and differential testing of histone marks

Since we observed that there is a strong enrichment of H3K4me3 reads in a region 4kb around the TSS (**Fig. S1D**) we quantified histone modification levels for all TSS by counting ChIP-seq reads aligned to each TSS region. We compared three biological replicates of experimental condition in order to determine differentially modified regions. The read count data was analyzed using a negative binomial (NB) regression model. The dispersion parameter of the NB model was estimated by mean-dependent local regression using DESeq, which was shown to be more appropriate for small numbers of biological replicates than maximum likelihood estimation (Anders and Huber, 2010). Subsequently, we adjusted p-values from the analysis for multiple testing using the Benjamini-Hochberg method (Klipper-Aurbach et al., 1995). We used this negative binomial regression framework of DESeq to test two hypothesis considering the two categorical variables high salt and LPS-stimulation. (1) We tested the effect of salt by comparing the full model histone ~ salt + LPS against the reduced model histone ~ LPS. (2) We tested whether the effect of salt is different depending on LPS-stimulation by comparing the full model histone ~ salt * LPS including an interaction term against the reduced model histone ~ salt + LPS.

Macrophage infection studies

For infection with *L. major*, BMM were co-cultured with *L. major* promastigotes at ratios from 1:30 for 4 h. Thereafter, extracellular *Leishmania* were washed off and the macrophages were further cultured in the presence of the indicated stimuli for a total of 72 h. The percentage of infected macrophages was determined microscopically after Diff-Quik[®] staining (Medion Diagnostics AG). For infection with *E. coli*, RAW264.7 macrophages were infected with *E. coli* HB101 with a multiplicity of infection of 10 for 1 h. After infection, cells were washed to remove extracellular bacteria. Gentamicin 100 $\mu\text{g} \times \text{ml}^{-1}$ (G100) was added to prevent replication of the remaining extracellular bacteria for 1 h, followed by 25 $\mu\text{g} \times \text{ml}^{-1}$ gentamicin (G25) in normal cell culture medium (NS: normal salt) or with additional 40 mM NaCl in the medium (HS: high salt) for the rest of the experiment. Infection was terminated by cellular lysis using 0.5% Triton X-100 in PBS, and the number of intracellular bacteria was determined by serial dilution in 0.05% Tween 20 in PBS and subsequent plating on Müller-Hinton plates. CFU were enumerated after incubation overnight at 37°C. For immunofluorescence studies, cells were infected with *E. coli* HB101 harboring pFV25.1 allowing for constitutive expression of GFPMut3a (Valdivia and Falkow, 1996). At indicated time points, cells were fixed with 3.5% paraformaldehyde (PFA). Staining was performed in a

blocking solution (1% BSA, 5% FCS in PBS) containing 0.1% saponin. Actin cytoskeleton was visualized using Phalloidin 546 (Invitrogen). Prolong Gold containing DAPI (Invitrogen) was used to visualize DNA and mount stained cells.

Infection of mice and determination of parasite burden

All animal experiments were carried out according to the protocols approved by the Animal Welfare Committee of the local government (Regierung von Mittelfranken, Ansbach, Germany). After two weeks on low salt diet (LSD; chow with <0.1% NaCl, tap water) or high salt diet (HSD; chow with 4% NaCl, 0.9% saline), we infected FVB mice (Charles River, Sulzbach) or LysM^{WT} *Nfat5*^{fl/fl} (control) and LysM^{Cre} *Nfat5*^{fl/fl} mice (FVB background; (Kueper, 2013; Wiig et al., 2013)) in their hind footpads with 3×10^6 of stationary-phase *L. major* promastigotes of a low *in-vitro* passage (≤ 5) in 50 μ l PBS. The respective diets were continued throughout the experiment. Footpad swelling was measured with a caliper. The number of parasites in the tissue was determined by limiting dilution analysis. Serial threefold dilution of tissue suspensions and 12 wells per dilution step were analyzed by applying Poisson statistics and the χ^2 -minimization method (L-Calc. software, Stemcell Technologies).

Analysis of NOS2 protein expression in the infected tissue

Single cell suspensions were obtained using gentle MACS (Miltenyi Biotec) according to the manufacturer's instructions. The single cell suspension was washed with PBS containing 2% FCS and stained for CD11b. Thereafter, the stained cells were fixed and permeabilized using BD Cytofix/CytopermTM Plus Fixation/Permeabilization Kit (with BD GolgiStopTM protein transport inhibitor containing monensin) and subsequently stained for NOS2. Data acquisition was performed FACS Canto II (BD Biosciences) and data were analyzed with FlowJo software (Tree Star).

***In vitro* restimulation with soluble *Leishmania* antigen**

As described elsewhere (Mahnke et al, 2014), single-cell suspensions from popliteal draining lymph nodes were prepared and restimulated with whole soluble *Leishmania* antigen (SLA). SLA was prepared by three freeze (-70°C) and thaw cycles and a final sonification step for 30 seconds (level 5, Branson Sonifier). After 3 days supernatants were collected, and IFN- γ was measured by enzyme linked immunosorbent assay (BD Biosciences).

Analysis of tissue *Nfat5* mRNA levels and macrophage infiltration

We extracted total RNA from mice skin with RNeasy Minicolumns (Qiagen, Hilden, Germany), homogenizing skin slices (~10-20 mg) in 500 μ l of RLT buffer reagent with an Ultra-Turrax for 30 s. After homogenization, we added 950 μ l of water and 16 μ l of proteinase K (25 U/ μ l), and incubated the sample at 55°C for 10 min followed by a centrifugation step (12,000 rpm for 3 min). After addition of 1 ml of 96–100% ethanol, we transferred the sample to the mini-columns and eluted according to the standard protocol. First-strand cDNA was synthesized with TaqMan RT reagents (Applied Biosystems, Darmstadt, Germany), with random hexamers used as primers. We performed real-time PCR with an ABI PRISM 7000 sequence detector and SYBR green reagents (Applied Biosystems, Darmstadt, Germany) according to the manufacturer's instructions. Primers used for amplification: fwd TGTTTCAGCCATTTACGTACACTCC, rev ACATTCAAAGCACCAGCTGCT. All samples were run in duplicates. We normalized the relative amount of the specific mRNA of interest with respect to 18S rRNA content in the sample. Dissociation curves confirmed the specificity of the PCR (Machnik et al, 2009).

We fixed tissues in formalin and embedded them in paraffin. We counted macrophages after staining with and CD68-specific antibody and visualized the stained cells with a secondary antibody labeled with Cy3 (from Jackson ImmunoResearch). Stained cells were mounted with Vectashield Mounting Medium containing DAPI (Vector). We counted macrophages at 200-fold magnification (high power field) and counted at least 5 HPF per section.

Electrolyte analysis

Chemical analysis of the carcasses included Na⁺, K⁺ and water measurements after dry ashing of tissues as reported previously (Machnik et al., 2009). Briefly, tissues were weighted (wet weight) and then desiccated at 80°C for 72 hours (dry weight). The difference between wet weight and dry weight was considered as tissue water content. After desiccation, the tissues were ashed at 200°C, 400°C, and 600°C for 24 hours at each temperature level and then dissolved in 5% HNO₃. Na⁺ and K⁺ concentrations were measured by atomic absorption spectrometry (Model 3100, Perkin Elmer). Plasma electrolytes and cell culture Na⁺ concentrations were analyzed with a clinical blood gas analyzer (Radiometer Copenhagen). Cell culture osmolality was determined by a vapor pressure VAPRO 5520 osmometer (Wescor).

²³Na MRI estimation of skin Na⁺ content in humans

We studied normal subjects and patients suffering from skin infection after due institutional review board approval according to the principles of the Declaration of Helsinki. All participants gave their written informed consent. Tissue Na⁺ content was assessed as described earlier (Kopp et al., 2012). ²³Na MRI was performed with a 3.0T clinical MR system (Verio, Siemens Healthcare) using a gradient echo sequence (2D-FLASH, total acquisition time (TA): 13.7 minutes, echo time (TE): 2.07 ms, repetition time (TR): 100 ms, flip angle (FA): 90°, 128 averages, resolution: 3x3x30mm³) and a frequency-adapted mono-resonant transmit/receive birdcage knee coil (32.602 MHz, Stark Contrast). ²³Na MRI grayscale measurements of aqueous standard solutions with increasing Na⁺ concentrations (10, 20, 30, and 40 mmol/L) served to calibrate relative tissue Na⁺.

²³Na spectroscopy of skin Na⁺ content in humans

A handmade double-resonant ¹H/²³Na surface coil (Stark-Contrast) for high resolution imaging and sodium spectroscopy of human lower leg skin was implemented using a 3.0 T MR-scanner (Verio, Siemens Healthcare). The coil consists of a 1 cm diameter ²³Na loop, a concentric 3.5 cm diameter ¹H loop and a 100 mM NaCl reference solution. A shift reagent (50 mM Tm[DOTP]⁵⁻, Macrocyclics) was added to the calibration solution to shift the resonance peak of the internal reference 35 - 40 ppm relative to the center-frequency of the skin-peak. The specifications allow for discrimination of the calibration (control) peak from the skin peak.

The ²³Na free induction decay was registered to acquire sodium spectra using TE = 450 ms, TE = 0.15 ms, TA = 1 min, FA = 90°, pulse duration 0.1 ms and bandwidth (BW) = 5 kHz. After fast fourier transform, integrals of reference and skin peaks of the magnitude spectrum were calculated by the scanners spectroscopy software (VD13, Siemens Healthcare, Erlangen, Germany). The ratio of the skin peak relative to the reference peak represents the amount of sodium within the 1/e-penetration depth of the ²³Na-loop, which is in the range of 2 mm when using a 40 V-excitation-pulse. To correlate skin-[Na] with skin thickness and spectral peak-ratios (PR) a calibration curve was established. As external calibration standards, we used agarose-layers (mimicking sodium containing epidermal skin tissue) with different thicknesses (0.4mm to 5 mm) and two sodium concentrations (50 mM and 100 mM).

To enable comparison of ²³Na MRI with ²³Na spectroscopy, lower legs skin of 19 healthy volunteers (age: 24-72 years, mean 51 ± 16 years, 11 males, 8 females) were measured with both techniques after due institutional review board approval (IRB) according

to the principles of the Declaration of Helsinki. Individuals were positioned feet-first and supine in the MR scanner with the left lower leg in the volume coil. After ^{23}Na imaging of the calf the volume, the coil was replaced by the $^1\text{H}/^{23}\text{Na}$ -surface coil to focus on the dorsal skin region by means of ^{23}Na spectroscopy.

References

- Anders, S., and Huber, W. (2010). Differential expression analysis for sequence count data. *Genome Biol* *11*, R106.
- Barski, A., Cuddapah, S., Cui, K., Roh, T.Y., Schones, D.E., Wang, Z., Wei, G., Chepelev, I., and Zhao, K. (2007). High-resolution profiling of histone methylations in the human genome. *Cell* *129*, 823-837.
- Bohm, C., Hayer, S., Kilian, A., Zaiss, M.M., Finger, S., Hess, A., Engelke, K., Kollias, G., Kronke, G., Zwerina, J., et al. (2009). The alpha-isoform of p38 MAPK specifically regulates arthritic bone loss. *J Immunol* *183*, 5938-5947.
- Jantsch, J., Wiese, M., Schodel, J., Castiglione, K., Glasner, J., Kolbe, S., Mole, D., Schleicher, U., Eckardt, K.U., Hensel, M., et al. (2011). Toll-like receptor activation and hypoxia use distinct signaling pathways to stabilize hypoxia-inducible factor 1{alpha} (HIF1A) and result in differential HIF1A-dependent gene expression. *J Leukoc Biol* *90*, 551-562.
- Klipper-Aurbach, Y., Wasserman, M., Braunspiegel-Weintrob, N., Borstein, D., Peleg, S., Assa, S., Karp, M., Benjamini, Y., Hochberg, Y., and Laron, Z. (1995). Mathematical formulae for the prediction of the residual beta cell function during the first two years of disease in children and adolescents with insulin-dependent diabetes mellitus. *Med Hypotheses* *45*, 486-490.
- Kopp, C., Linz, P., Wachsmuth, L., Dahlmann, A., Horbach, T., Schofl, C., Renz, W., Santoro, D., Niendorf, T., Muller, D.N., et al. (2012). ²³Na magnetic resonance imaging of tissue sodium. *Hypertension* *59*, 167-172.
- Kueper, C., Beck, F.X., Neuhofer, W. (2013). Cytokine Expression during Sepsis Is Repressed in Conditional NFAT5-knockout Mice. *J Am Soc Nephrol* *24*, 306A.
- Landt, S.G., Marinov, G.K., Kundaje, A., Kheradpour, P., Pauli, F., Batzoglou, S., Bernstein, B.E., Bickel, P., Brown, J.B., Cayting, P., et al. (2012). ChIP-seq guidelines and practices of the ENCODE and modENCODE consortia. *Genome Res* *22*, 1813-1831.
- Li, H., Handsaker, B., Wysoker, A., Fennell, T., Ruan, J., Homer, N., Marth, G., Abecasis, G., and Durbin, R. (2009). The Sequence Alignment/Map format and SAMtools. *Bioinformatics* *25*, 2078-2079.
- Machnik, A., Neuhofer, W., Jantsch, J., Dahlmann, A., Tammela, T., Machura, K., Park, J.K., Beck, F.X., Muller, D.N., Derer, W., et al. (2009). Macrophages regulate salt-dependent volume and blood pressure by a vascular endothelial growth factor-C-dependent buffering mechanism. *Nat Med* *15*, 545-552.
- Mahnke, A., Meier, R.J., Schatz, V., Hofmann, J., Castiglione, K., Schleicher, U., Wolfbeis, O.S., Bogdan, C., and Jantsch, J. (2014). Hypoxia in Leishmania Major-Skin Lesions Impairs the NO-Dependent Leishmanicidal activity of Macrophages. *J Invest Dermatol*.

Neufert, C., Becker, C., Wirtz, S., Fantini, M.C., Weigmann, B., Galle, P.R., and Neurath, M.F. (2007). IL-27 controls the development of inducible regulatory T cells and Th17 cells via differential effects on STAT1. *Eur J Immunol* 37, 1809-1816.

Ruzankina, Y., Pinzon-Guzman, C., Asare, A., Ong, T., Pontano, L., Cotsarelis, G., Zediak, V.P., Velez, M., Bhandoola, A., and Brown, E.J. (2007). Deletion of the developmentally essential gene ATR in adult mice leads to age-related phenotypes and stem cell loss. *Cell Stem Cell* 1, 113-126.

Schleicher, U., and Bogdan, C. (2009). Generation, culture and flow-cytometric characterization of primary mouse macrophages. *Methods Mol Biol* 531, 203-224.

Stenger, S., Donhauser, N., Thuring, H., Rollinghoff, M., and Bogdan, C. (1996). Reactivation of latent leishmaniasis by inhibition of inducible nitric oxide synthase. *J Exp Med* 183, 1501-1514.

Valdivia, R.H., and Falkow, S. (1996). Bacterial genetics by flow cytometry: rapid isolation of *Salmonella typhimurium* acid-inducible promoters by differential fluorescence induction. *Mol Microbiol* 22, 367-378.

Wiese, M., Castiglione, K., Hensel, M., Schleicher, U., Bogdan, C., and Jantsch, J. (2010). Small interfering RNA (siRNA) delivery into murine bone marrow-derived macrophages by electroporation. *J Immunol Methods* 353, 102-110.

Wiig, H., Schroder, A., Neuhofer, W., Jantsch, J., Kopp, C., Karlsen, T.V., Boschmann, M., Goss, J., Bry, M., Rakova, N., et al. (2013). Immune cells control skin lymphatic electrolyte homeostasis and blood pressure. *J Clin Invest* 123, 2803-2815.

Wittmann, I., Schonefeld, M., Aichele, D., Groer, G., Gessner, A., and Schnare, M. (2008). Murine bactericidal/permeability-increasing protein inhibits the endotoxic activity of lipopolysaccharide and gram-negative bacteria. *J Immunol* 180, 7546-7552.